

PAPER • OPEN ACCESS

Formation of micro-plumes at a planar solid/liquid interface in a temperature gradient

To cite this article: J P Mogeritsch *et al* 2019 *IOP Conf. Ser.: Mater. Sci. Eng.* **529** 012025

View the [article online](#) for updates and enhancements.



IOP | ebooks™

Bringing you innovative digital publishing with leading voices to create your essential collection of books in STEM research.

Start exploring the collection - download the first chapter of every title for free.

Formation of micro-plumes at a planar solid/liquid interface in a temperature gradient

J P Mogeritsch, T Peifer and A Ludwig

Department of Metallurgy, Chair for Simulation and Modelling Metallurgical Processes, Montanuniversitaet Leoben, Austria

*Corresponding author: johann.mogeritsch@unileoben.ac.at

Abstract: For directional solidification experiments with low withdrawal rates near and even below the constitutional undercooling limit of the corresponding alloy, a sample is needed which reveals a homogeneous concentration along the sample axis. As stirring in samples of a certain length is difficult, homogenization by rapid solidification is very common. Hereby, the liquid sample is rapidly moved from hot to cold and thus fine and long dendrites with segregated interdendritic liquid are formed. By subsequently melting and holding the sample in a resting position within a given temperature gradient, diffusion in the liquid and enhanced diffusion in the hot solid diminishes local concentration differences. In this paper, we report on homogenization and solidification experiences with transparent organic model compounds of TRIS-NPG. During one hour of homogenization we observed (i) formation of a coarse grain structure, (ii) liquid film and droplet migration by temperature gradient zone melting, and (iii) formation and eventually disappearance of liquid channels. During solidification experiments we occasionally found liquid channels, which revealed a connection to the solid/liquid interface; liquid that rose in the channel and thus formed micro-plumes at the planar solid/liquid interface. This upwards motion is explained by solutal buoyancy of NPG-rich liquid and a possible feeding through an interconnected network of channels.

Keywords: organic model system, peritectic layered structures, Bridgman-furnace, plumes, thermos-solutal convection

1. Introduction

The interesting characteristic in peritectic systems is the possibility of forming peritectic layered structures around the peritectic temperature T_p . For a peritectic reaction, a solid primary phase α and a liquid phase L reacts during cooling to form a second solid peritectic phase β ($\alpha + L \rightarrow \beta$). Close to or below the limit of constitutional undercooling peritectic layers are possible as a result of a competitive growth of both phases directly from the melt [1, 2]. Since the formation of such peritectic layered structures is highly influenced by convection in the melt, sample thicknesses in the range of μm are often used as those flat containments suppress fluid flow to a large extent. Using the Bridgman technique, the organic model system TRIS-NPG [3] has been used by the authors for in-situ observation of the dynamics of the solid/liquid (s/l) interface which leads to layered peritectic solidification morphologies [4-13].

Often concentration homogenization in such samples is performed by fast melting and rapid solidification which in turn leads to a fine dendritic structure. Afterwards when the sample is stopped, the temperature gradient leads to local remelting and solidification phenomena [14-19]. These processes involved morphological changes and coarsening, as well as macroscopic mass transport, migration of liquid droplets and liquid film migration through the solid matrix, known as temperature gradient zone melting (TGZM) [14].

To deepen our understanding, investigations were performed to visualize the influence of convection in the melt and migration movements in the solid on the formation of layered peritectic structures by using seeding particles as tracers [20].

2. Experimental set-up

Our Bridgman-furnace for in-situ observation consists of a hot zone of 10 mm and a cold zone of 40 mm departed by an adiabatic observation gap of 7 mm. The moving slide to pull the glass sample through the furnace is located about 40 mm below the cold zone and the sample stands out up to 100 mm above



the outer rim of the hot zone after fixing. The two organic substances TRIS and NPG were obtained as a powder with a purity of 99% for NPG and 99.9+ % for TRIS. Both substances exhibit a faceted low temperature phase and an orientationally disordered crystalline high temperature phase, called "plastic phase". In order to visualize the flow pattern tracers in the form of hollow glass spheres seeding particles [21] with an average distribution size of $11 \pm 9 \mu\text{m}$ were added to the organic substances. We produced the organic components by melting and cooling together both components in the appropriate composition together with the particles. A glass tube sample (length $\sim 200 \text{ mm}$) was filled with the seeding-enriched component by capillary force. Within the Bridgman-furnace, the sample was illuminated through the adiabatic zone to observe the forming solidification morphology with a light transmission microscope. Images were recorded by a CCD camera for a subsequent evaluation. More details concerning the sample preparation and the experimental set-up are given in [6, 8].

In-situ investigations were carried out by placing the sample within the preheated Bridgman-furnace. The temperature gradient G_T within the adiabatic area was controlled by the selected temperature of the hot and cold zone of the furnace. For the experiments presented in this paper the gradient was measured with a fine thermocouple within a constantly moving, filled sample to be $G_T = 5.6 \text{ K/mm}$. Once the sample was connected with the pulling device it was drawn through the furnace from hot to cold with a relatively fast velocity of $V = 15.7 \mu\text{m}\cdot\text{s}^{-1}$ for 50 minutes. It should be noted that in this time period approximately 47 mm sample length are pulled through the 10 mm width hot zone. The organic component melts when entering the hot zone and solidifies within the adiabatic gap again. Finally, the sample remains still in the furnace for 60 minutes before the solidification experiments with a pulling velocity rate of $V = 0.174 \mu\text{m}\cdot\text{s}^{-1}$ for several hours was carried out.

Here, we have recorded the processes which are activated by the selected homogenization method and observed the corresponding influence on the formation of layered structures for a hyper-peritectic alloy of $x = 0.52 \text{ mol fraction NPG}$.

3. Results

At room temperature, the organic component only displayed the faceted face. By placing the sample within the Bridgman-furnace the faceted phase rapidly melt or transformed partly into the plastic phase, see figure 1a, depending on the position within the adiabatic zone. The s/l interface showed a convex surface towards the two sideward glass walls during the melting process - an effect caused by the small variation in the heat conductivity of the glass sample and the organic component.

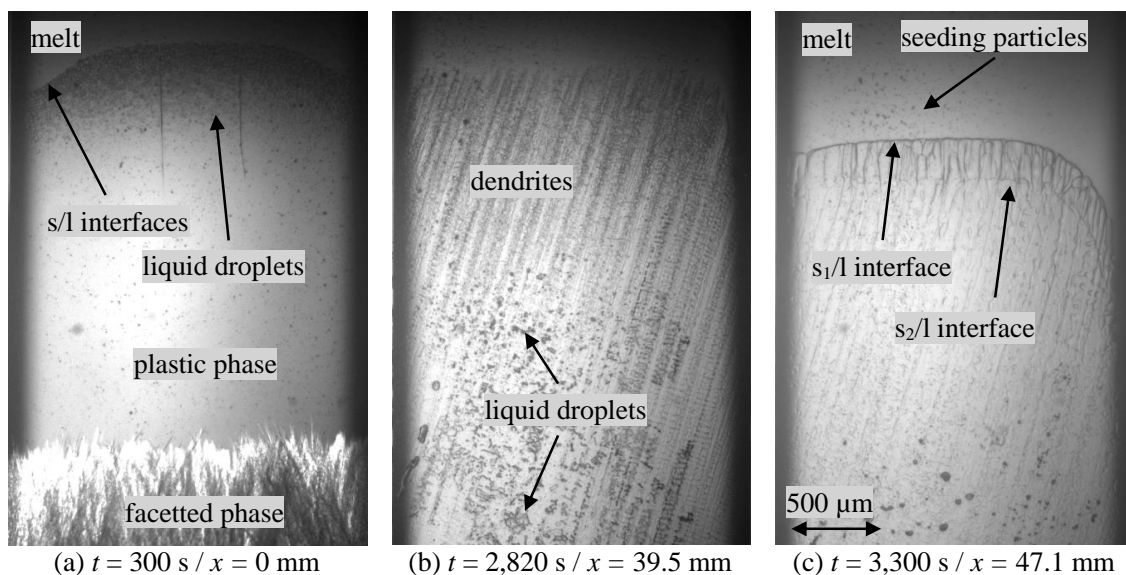


Figure 1: (a) Partial melting of the organic substance while the sample remains at rest. (b) Dendritic solidification structure while the sample is pulled through the temperature gradient with $V = 15.7 \mu\text{m}\cdot\text{s}^{-1}$. (c) Solidification morphology after one hour at rest. Two interfaces at different temperature levels are formed. The dark shadow on the pictures left and right side originates by the side glass walls. Below the pictures the experimental time and the solidification length are given.

The transparent plastic phase displayed a bubble-like structure close to the s/l interface which disappeared within minutes by further melting. The remaining faceted phase showed a filamentous structure. As soon as the sample was fixed to the pulling device ($\Delta t \sim 5$ minutes) and before the thermodynamic equilibrium was reached, it was moved through the temperature gradient at a velocity of $V = 15.7 \mu\text{m}\cdot\text{s}^{-1}$.

Due to the enforced solidification, the s/l interface changed into dendritic solidification morphology, see figure 1b. After around 50 minutes, which corresponded to a solidification length of 47.1 mm, the process was stopped and the sample was kept at the same position for one hour to achieve thermal stability. During this period, the morphological structure transformed from dendritic to planar and two boundary layers were formed at different temperature levels - one planar s/l interface, labelled s_1/l , and a second one, terms s_2/l , at a lower temperature level compare to s_1/l (figure 1c).

After 1 hour at rest, the sample was pulled (specified solidification time $t = 0$ s) with $V = 0.174 \mu\text{m}\cdot\text{s}^{-1}$ and both interfaces recoiled to a lower temperature level. Simultaneously, movement of the particles in the melt exhibited a descending flow in the middle of the sample and an upward motion along the two lateral glass walls. Particles from liquid films connected to the s_1/l interface rose up into the melt and formed several temporary micro-plumes.

After $\Delta t = 3,600$ s, as the s_1/l interface passed the initial position of the s_2/l interface, the growth of a new phase was observed. This happened on the sample's right side where the new phase in form of a band grew laterally towards the center of the sample. Subsequently, a new band began to grow laterally towards the center of the sample, coming in from the left side (see figure 2a).

During the formation of the bands, an enduring strong upward flow compare to the downwards flow in form of a micro-plume near the center of the sample was observed. Its strength was sufficient to change the flow direction in the sample (figure 2b) to an upward movement slightly offset from the center and a downward movement along the sidewall of the glass tube.

Shortly before the bands merged the initial phase is the new preferred phase and start to grow dominantly again. It spreads out in both lateral directions which can be recognized in the form of a growing triangle. Whereby, the lateral growth was hampered on the left side by the above-mentioned micro-plume. Simultaneously, a new band was formed on the right side of the sample. In contrast to the first band, the new phase grew in between the front and back of the existing phase and the glass wall (figure 2c). It expands toward the left side until it was stopped at the micro-plume. The growth of these bands constrained the existing phase in such a way that this led to peritectic coupled growth (PCG) on the right side of the sample. In contrast, the s/l interface at the center became unstable and cellular growth occurred. The left side was unaffected and the s/l interface grew planar (see figure 2d).

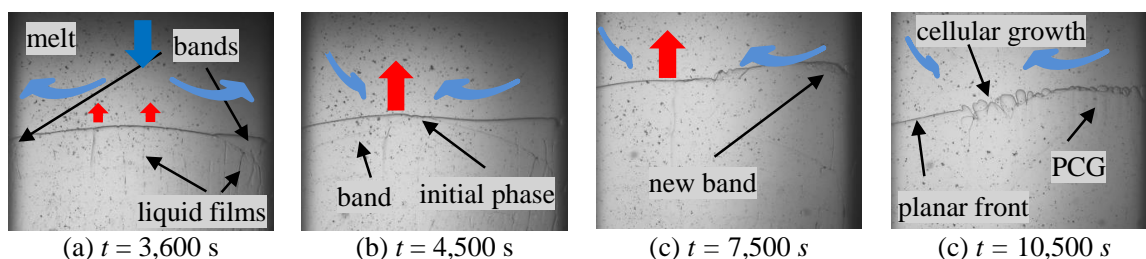


Figure 2: (a) Two bands form close to the sample side walls. (b) The original phase is again preferred. (c) A new band forms at the right side and the planar front becomes unstable at the center. (d) Transition from banded structure to peritectic coupled growth (PCG). Convection: The arrows show the flow in the melt and the micro-plumes. The width of the picture is $2,000 \mu\text{m}$.

4. Discussion

Since the mushy zone was formed via directed rapid solidification, elongated fine dendrites and corresponding interdendritic liquid developed. Particles were frozen in the solid structure of the initial dendrites or trapped within the interdendritic liquid (figure 3a). As soon as the sample became stable, a series of complex processes occurred. The dendrites widened and grew together and a planar s/l interface formed. Since the mushy zone was within a temperature gradient, liquid inclusions migrated in the solid phase toward higher temperatures up to the melt (figure 3b and c). Careful observation of the migration showed that the initial dendrite tips have grown at two different temperature levels and in different

depths of the sample. This fact was not observable during the rapid solidification process due to the transparent nature of the organic components. It seems to be that due to the fast solidification rate, dendrites consisting of the primary α phase in the center of the sample depth and the peritectic β phase close to the front glass wall were formed. As a consequence, two planar interfaces at different temperature levels were generated (figure 3c).

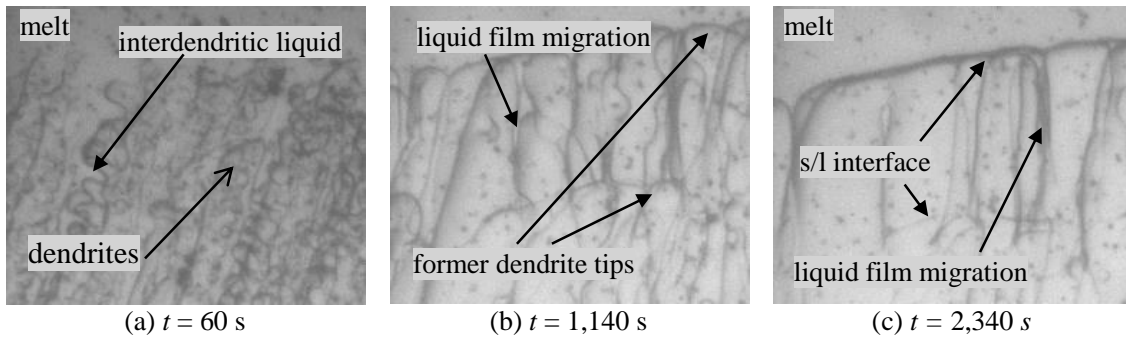


Figure 3: Sample in rest (a-c): migration of liquid inclusions and formation of two s/l interfaces. The width of the picture is 500 μm .

After one hour in rest, the solid was still full of liquid films. According to the phase diagram, the enclosed liquid must be enriched in NPG. Whereby, the density of the liquid decrease with the amount of NPG. Note, that the lower the temperature level, the higher the NPG content in the trapped liquid. Due to the migration of the liquid film within the temperature gradient, temporarily, liquid channels were formed by connecting various liquid films at different temperature levels up to the melt. Whereby, feeding through a liquid film network is postulate, high NPG-enriched liquid rises upwards through the liquid channels towards the melt forming micro-plumes. Just such a channel leads to the formation of the special plume as described in the previous chapter.

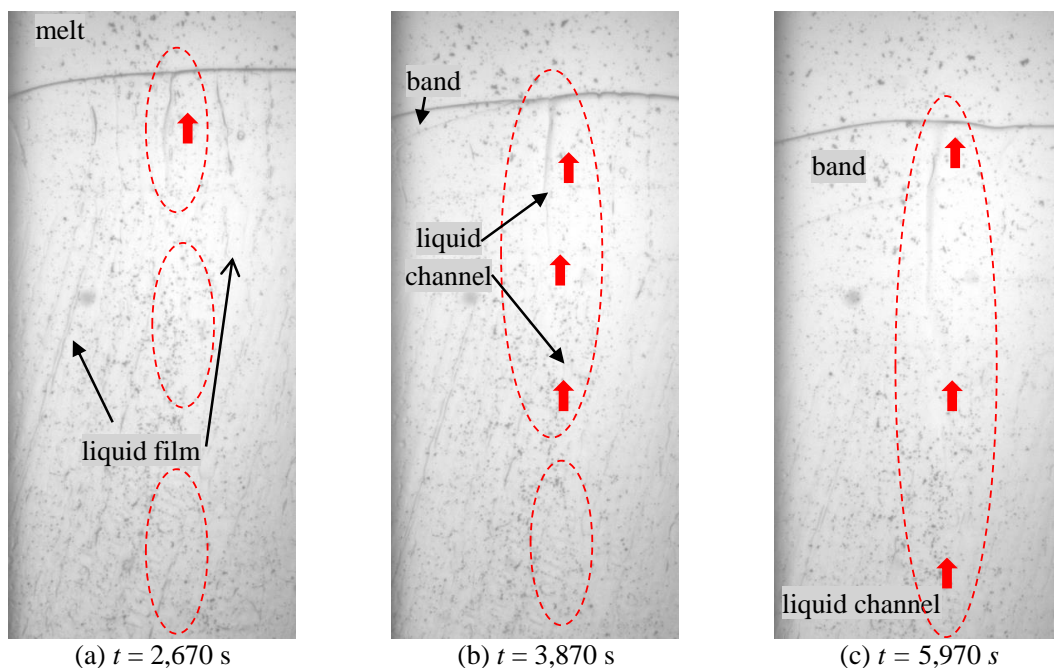


Figure 4: Formation of a long channel by connecting several liquid films (circles). Particle within the liquid channel are moving upwards (arrows) into the melt. The width of the picture is 1000 μm .

Figure 4 shows the formation of such a channel and the corresponding movement of particles within a time period of $\Delta t = 3,300$ s. This liquid channel formed a length of approx. 1,500 μm deep in the solid phase. The fluid channels were particularly recognizable by the particles moving therein. Whereby, at

this temperature level only concentrations close to pure NPG are still liquid. In contrast to particles in the bulk melt, the particles within the liquid channel kind of shoot out into the bulk melt. This upward flow was sufficient to alter the flow pattern in the melt as shown in figure 2a and b.

The position of the observed micro-plumes, the liquid flow direction, and the interpretation of the micro structure formation is shown in figure 5. Initially, there were two solid phases present, recognized as the α and β phases, respectively. Ahead of the interface, thermosolutal convection initiated a downward movement in the center and a corresponding upward motion along the sample side walls. For the given solidification rate, both interfaces tried to reach stable growth conditions at the corresponding solidus temperature; therefore, both s/l interfaces started to recoil. As soon as the s/l interface of the α phase (s_1/l) had passed the initial temperature level of the β phase (s_2/l), the peritectic phase started to grow in form of two band (figure 5a). Additionally, the liquid channel described in figure 4 was formed and the strong micro-plume was established. Whereby, it was not possible to detect a direct influence of the micro-plume on the peritectic band. However, as a consequence of the micro-plume, a new convection pattern in the melt was induced. During the growth of the peritectic phase on both sides, the micro-plume is still active (figure 5b). Shortly prior to the two β phase bands merging at the center, the α phase became again the preferred phase. This can be seen by the expanded laterally growing triangle. The growth of the initial primary phase from the center to the left edge was halted as the α -phase came into contact with the micro-plume. Unlike the spread of the peritectic phase, here, the flow prevented the lateral growth of the α phase. Simultaneously, a new α phase band appeared on the right side of the sample (figure 5c). The phase seems to be formed by nucleation at the β/l interface close to the wall. Since the α phase had grown between the glass wall and the existing β phase, the peritectic phase became enveloped by the primary phase except at the top. This circumstance led to a competing growth between the two phases in form of PCG, cellular growth in the center, and planar growth on the left side.

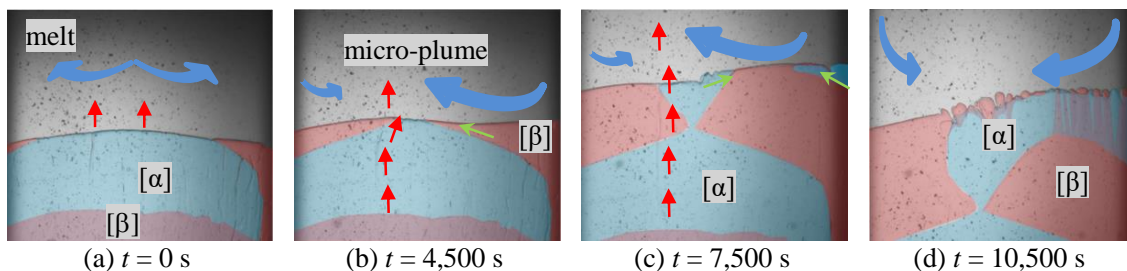


Figure 5: (a) Formation of two β island bands unaffected by the liquid flow of NPG-enriched plumes (arrows). The dots in the pictures are the seeding particles and the arrows indicate the thermosolutal convection at the front of the s/l interface. (b) Shortly before both β -island bands was going to merge the α phase became the new preferred phase. (c) The α phase formed a new band coming from the right side. The new band solidifies in a planar manner. The lateral growth of the α phase growing at the center is stopped on the left side by the micro plume. (d) A planar, cellular, and peritectic coupled growth front was formed. The width of the picture is 2,000 μm .

5. Conclusion

Solidification experiments to investigate peritectic layered structures were carried out with the transparent peritectic modelling system TRIS-NPG. In order to visualize the thermosolutal convection flow, seeding particles were added to the organic substances as tracers. We have managed to demonstrate that the rapid solidification led to a simultaneous growth of α and β phases in form of fine dendrites. The corresponding interdendritic fluid was, accordingly, NPG-enriched. Once the sample was at rest, the dendrites broadened to form a solid matrix and the interdendritic fluid became trapped in the form of liquid films and few droplets. Since there was a temperature gradient, the trapped liquid began to migrate by local melting and remelting. This migration remained at the beginning of the solidification experiment. As a result, several liquid films merged to one liquid channel connecting to the s/l interface. Due to the density difference, the liquid enclosed in this channel flowed upwards towards the bulk melt and formed a special micro plume there. This flow phenomenon was sufficiently strong to change the convection pattern in the melt. For the observed formation of peritectic layered structures, first, no interaction of the liquid channel with the corresponding special micro plume was observed. In the further course

of peritectic layered solidification, however, a direct influence of the liquid channel and micro plume on the solidification pattern was found.

Acknowledgements

This research has been supported by the Austrian Research Promotion Agency (FFG) within the framework of the METTRANS projects and by the European Space Agency (ESA) a part of the METCOMP project.

References

- [1] Boettinger W J 1974 The structure of directionally solidified two-phase Sc-Cd peritectic alloys, *Met. Trans.* **5** 2023–2031
- [2] Trivedi R 1995 Theory of layered-structure formation in peritectic systems, *Metal. Mater. Trans.* **26** (6) 1583-90
- [3] Barrio M, Lopez D O, Tamarit JL, Negrier P and Haget Y 1995 Degree of miscibility between non-isomorphous plastic phases: Binary system NPG -TRIS *J. Mater. Chem.* **5** 431-39
- [4] Ludwig A, Mogeritsch J 2011 In-situ observation of coupled peritectic growth, *Solidification Sci. Tech.: John Hunt Int. Symp.* 233-42
- [5] Mogeritsch J, Ludwig A 2011 In-situ observation of coupled growth morphologies in organic peritectics, *IOP Conf. Ser. Mater. Sci. Eng.* **7** 12028
- [6] Ludwig A, Mogeritsch J, Grasser M 2012 In-situ observation of unsteady peritectic growth modes, *Trans. Indian Inst. Metals* **62** 433-436
- [7] Mogeritsch J, Ludwig A 2012 Microstructure formation in the two phase region of the binary peritectic organic system TRIS-NPG, TMS Annual Meeting Symposium, *Materials Res. Microgravity*, Orlando, Florida, USA 48-56
- [8] Ludwig A, Mogeritsch J 2014 Recurring instability of cellular growth in a near peritectic transparent NPG-TRIS alloy system, *Mater. Sci. Forum* **790** 317-22
- [9] Mogeritsch J, Ludwig A 2015 In-situ observation of the dynamic of peritectic coupled growth using the binary organic system TRIS-NPG, *IOP Conf. Ser. Mater. Sci. Eng.* **84** 12055
- [10] Ludwig A, Mogeritsch J 2016 Compact seaweed growth of peritectic phase on confined, flat pro-peritectic dendrites, *J. Crystal Growth* **455** 99-104
- [11] Ludwig A, Mogeritsch J, Pfeifer 2017 In-situ observation of coupled peritectic growth in a binary organic model alloy *Acta. Mat.* **126**, 329-335
- [12] Mogeritsch J, Ludwig A 2018 Investigation on Peritectic Layered Structures by using the Binary Organic Components TRIS-NPG as Model Substances for Metal-Like Solidification, *Crimson Publishers, Res. Dev. Mater. Sci.* **4(1)** 1-3
- [13] Mogeritsch J, Ludwig A 2018 In-situ observation of growth morphologies in organic peritectics, ICTIMESH-18, Dubai, submitted
- [14] Pfann WG 1955 Temperature gradient zone melting, *J. Minerals, Metals & Materials Society* **7(9)** 961–964
- [15] Tiller W A 1963 Migration of a liquid zone through a solid: Part I, *J. Appl. Phys.* **34** 2757–2762
- [16] Rettenmayr M 2009 Melting and remelting phenomena, *Inter. Mater. Rev.* **54(11)** 1-17
- [17] Jabbareh M A, Assadi H 2009 Modelling of microstructure evolution in transient-liquid phase diffusion bonding under temperature gradient, *Scripta Mater.* **60** 780–782
- [18] Liu D, Li X, Su Y, Rettenmayr M, Guo J, Fu H 2014 Local melting/solidification during peritectic solidification in a steep temperature gradient: analysis of a directionally solidified Al–25at%Ni, *Appl. Phys. A* **116(4)** 1821–1831
- [19] Li Y j, Wang L, Ni P, Tan Y 2017 Growth of bulk Si from Si-Al alloy by temperature gradient zone melting, *Mater. Sci. Semicond. Process* **66** 170–175
- [20] Mogeritsch J P, Pfeiler T, Ludwig A 2018 Investigation on the Liquid Flow ahead of the Solidification Front During the Formation of Peritectic Layered Solidification Structure, *7th Int. Conf. on Solidification and Gravity*, University of Miskolc 319-324
- [21] Information on <https://www.dantecdynamics.com>